Tensor Reconstruction-Based Sparse Array Interpolation for 2-D DOA Estimation of Coherent Signals

Md. Saidur R. Pavel [†], Yimin D. Zhang [†], and Braham Himed [‡]

[†] Department of Electrical and Computer Engineering, Temple University, Philadelphia, PA 19122, USA
[‡] Distributed RF Sensing Branch, Air Force Research Laboratory, WPAFB, OH 45433, USA

***Abstract*—This paper proposes a tensor-based two-dimensional (2-D) direction-of-arrival (DOA) estimation method for coherent sources using a 2-D coprime array. The proposed method preserves the structural characteristics of multi-dimensional signals with multiple snapshots by constructing a covariance tensor of the received signal. To address the issue of rank-deficiency of the covariance tensor due to the coherency of the impinging signals, a structural tensor reconstruction method is employed to decorrelate the covariance tensor. Additionally, the use of a coprime array results in a non-contiguous difference coarray, leading to missing measurements in the reconstructed covariance tensor. To fully leverage the aperture provided by the coprime array, the missing correlations are interpolated by solving a convex optimization problem. The canonical polyadic decomposition method is applied to the interpolated covariance tensor to detect the coherent sources. The conditions for source resolvability are also analyzed.**

Keywords*—*Direction-of-arrival estimation, sparse array, tensor decomposition, canonical polyadic decomposition, coherent signals

I. Introduction

Direction-of-arrival (DOA) estimation is a key technology in array signal processing that determines the spatial spectrum of impinging signals. It has broad applications in wireless communication, radar, automotive vehicles, sonar, radio astronomy, and biomedical imaging [1–6]. Subspace-based methods, such as MUSIC [7] and ESPRIT [8], are popularly used for DOA estimation due to their superior performance and low complexity. However, when dealing with coherent signals, these methods suffer from the rank-deficiency problem and fail to resolve their DOAs without proper decorrelation. Coherent signals are frequently encountered in practice, including multi-path propagation, low-grazing-angle scattering, and reflection signals from swarm targets.

By using two-dimensional (2-D) arrays, both azimuth and elevation angles can be estimated. Compared to the one-dimensional counterpart for coherent signals, 2-D DOA estimation for coherent signals is even more challenging. DOA estimation methods developed for coherent signal detection exploiting linear arrays primarily rely on matrix-based processing. These approaches require transformation of the array data in a vector form into a covariance matrix when utilizing multiple data snapshots. An effective way to preserve and utilize the inherent structural properties of multi-dimensional signals associated with a 2-D array is to use tensor modeling, and tensor decomposition techniques can be used to effectively exploit the inherent characteristics of such signals. Commonly used tensor decomposition methods include canonical polyadic decomposition (CPD) [9, 10], Tucker decomposition [11], and high-order singular value decomposition (HOSVD) [12]. For example, tensor decomposition is used in [13] for DOA estimation using multiple-invariance sensor array processing. In [14], a coarray tensor DOA estimation approach is developed to utilize augmented co-coarrays of multi-dimensional structured sparse arrays. It is worth noting that these methods primarily address uncorrelated sources. To handle coherent signals, tensor-based spatial smoothing techniques are presented in [15] and [16]. Nevertheless, these methods involve repeated tensor calculations, resulting in limited decorrelation effectiveness and a substantial computational burden. In [17], a tensorial Hermitian Toeplitz structure is reconstructed from the coherent covariance tensor utilizing its structural property.

Compared to uniform arrays, sparse arrays offer an enlarged array aperture and a higher number of degrees-of-freedom (DOFs). Recently, systematic sparse array designs, inspired by the nested array [18] and the coprime array [19, 20], become attractive to ensure effective sparse array design and performance analysis. Various signal processing techniques are developed to perform DOA estimation exploiting such structured sparse arrays [21–24] where augmented virtual arrays derived from second-order statistics are used to enhance the available DOFs.

In this paper, we consider the CPD tensor decomposition approach for 2-D DOA estimation of coherent signals exploiting 2-D coprime arrays. To decorrelate the covariance tensor obtained from coherent signals, a structured tensor reconstruction method is employed. Due to the partially augmented nature of the coprime array, there are missing measurements, also referred to as holes, in its difference coarray, leading to discontinuities in the derived virtual array. These holes in the difference coarray also result in missing elements in the reconstructed covariance tensor. To address this issue and fill these holes in the decorrelated covariance tensor, we employ a coprime array interpolation technique [25] to estimate the unknown correlations of the decorrelated covariance tensor. By applying CPD to the interpolated and decorrelated covariance tensor, 2-D DOAs of the coherent sources are estimated. The effectiveness of the proposed technique is validated through theoretical analyses and simulation results.

Notations: We use lower-case bold characters (e.g., $\boldsymbol{a}$), upper-case bold characters (e.g., $\boldsymbol{A}$), and upper-case calligraphic bold characters (e.g., $\boldsymbol{\mathcal{A}}$) to denote vectors, matrices, and tensors, respectively. In particular, $\boldsymbol{\mathcal{I}}$ denotes the identity matrix of a proper dimension. $(\cdot)^{\mathrm{T}}$ and $(\cdot)^{\mathrm{H}}$ respectively

This material is based upon work supported by the Air Force Office of Scientific Research under award number FA9550-23-1-0255. Any opinions, findings, and conclusions or recommendations expressed in this material are those of the authors and do not necessarily reflect the views of the United States Air Force.

represent the transpose and Hermitian operations of a matrix or vector. $\circ$ denotes the outer product and $\odot$ denotes the Hadamard product. In addition, $\text{vec}(\cdot)$ vectorizes a matrix, $\kappa(\cdot)$ represents the Kruskal rank of a matrix, and $\text{triu}(\cdot)$ and $\text{tril}(\cdot)$ represent the upper and lower triangular elements of a matrix, respectively. $\mathbb{E}[\cdot]$ stands for the statistical expectation operator. $\mathcal{R}(\cdot)$ extracts the real part of a complex entry, and $\mathbb{C}^{I_1 \times I_2 \times \cdots \times I_N}$ denotes the complex space with the specified dimension. $|\mathbb{P}|$ returns the cardinality of set $\mathbb{P}$. $\mathcal{T}(\boldsymbol{x})$ denotes a Hermitian Toeplitz matrix with $\boldsymbol{x}$ as its first column and $\text{Tr}(\cdot)$ represents the trace operator.

CPD: CPD represents a high-order tensor as a linear combination of a minimum number of rank-1 tensor components. For an N-dimensional tensor $\boldsymbol{\mathcal{A}} \in \mathbb{C}^{I_1 \times I_2 \times \cdots \times I_N}$, its rank-$R$ CPD is expressed as

$$\boldsymbol{\mathcal{A}} = \sum_{r=1}^{R} \eta_r \boldsymbol{a}_1(r) \circ \boldsymbol{a}_2(r) \circ \boldsymbol{a}_N(r) \triangleq [\![\boldsymbol{\eta}; \boldsymbol{A}_1; \boldsymbol{A}_2; \boldsymbol{A}_N]\!], \quad (1)$$

where $\boldsymbol{a}_n(r) \in \mathbb{C}^{I_n}$ is a canonical polyadic (CP) factor, $\boldsymbol{A}_n = [\boldsymbol{a}_n(1), \boldsymbol{a}_n(2), \cdots, \boldsymbol{a}_n(R)] \in \mathbb{C}^{In \times R}$ denotes the corresponding factor matrix for $n = 1, 2, \cdots, N$, and $\boldsymbol{\eta} = [\eta_1, \eta_2, \cdots, \eta_R]^{\text{T}}$ is a vector of scalar coefficients.

II. Array and Signal Models

A. Array Geometry Model

Consider an origin-centric coprime planar array $\mathbb{S}$ consisting of two sparse subarrays with a uniform rectangular array (URA) configuration, respectively denoted as $\mathbb{M}$ and $\mathbb{N}$, where $\mathbb{S} = \mathbb{M} \cup \mathbb{N}$. There are $M_x \times M_y$ sensors in the sparse subarray $\mathbb{M}$ and $N_x \times N_y$ sensors in the sparse subarray $\mathbb{N}$, as depicted in Fig. 1, where (M_x, N_x) and (M_y, N_y) are positive coprime integer pairs. The inter-element spacing for the sparse subarray $\mathbb{M}$ is $N_x d$ and $N_y d$ along the X and Y axes, respectively, where $d = \lambda/2$ with λ denoting the signal wavelength. Similarly, the inter-element spacing for sparse subarray $\mathbb{N}$ is $M_x d$ and $M_y d$ along the X and Y axes, respectively. Without loss of generality, we assume that the number of sensors in each direction is an odd integer for both subarrays.

For subarrays $\mathbb{M}$ and $\mathbb{N}$, the sensors are positioned at

$$\begin{aligned} \mathbb{P}_{\mathbb{M}} &= \{(x_{\mathbb{M}}, y_{\mathbb{M}}) \mid x_{\mathbb{M}} \in N_x m_x d, y_{\mathbb{M}} \in N_y m_y d\}, \\ \mathbb{P}_{\mathbb{N}} &= \{(x_{\mathbb{N}}, y_{\mathbb{N}}) \mid x_{\mathbb{N}} \in M_x n_x d, y_{\mathbb{N}} \in M_y n_y d\}, \end{aligned} \quad (2)$$

respectively, where

$$\begin{aligned} -(M_x - 1)/2 \le m_x \le (M_x - 1)/2, \\ -(M_y - 1)/2 \le m_y \le (M_y - 1)/2, \\ -(N_x - 1)/2 \le n_x \le (N_x - 1)/2, \\ -(N_y - 1)/2 \le n_y \le (N_y - 1)/2. \end{aligned}$$

The location of sensors for the planar array $\mathbb{S}$ can then be expressed as

$$\mathbb{P} = \mathbb{P}_M \cup \mathbb{P}_N. \quad (3)$$

Due to the coprime relationship, the sensors in subarrays $\mathbb{M}$ and $\mathbb{N}$ do not overlap except at the origin. Hence, the total number of sensors is $M_x M_y + N_x N_y - 1$.

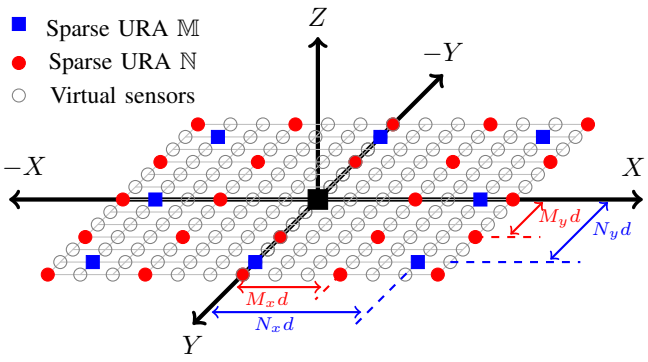

Fig. 1: Array configuration

B. Signal Model

Consider L narrowband far-field coherent signals impinging on the planar array $\mathbb{S}$ from azimuth and elevation angles (θ_l, ϕ_l), $l = 1, 2, \cdots, L$. These L coherent signals are a scaled version of $s(t)$ up to a complex scalar α_l.

Denote $\mu = \sin(\phi)\cos(\theta)$ and $\nu = \sin(\phi)\sin(\theta)$. Then, the steering vectors for subarray $\mathbb{M}$ in the X and Y directions are respectively expressed as

$$\begin{aligned} \boldsymbol{a}_{\mathbb{M}}(\mu) &= [e^{-j\pi \frac{-(M_x-1)}{2} N_x \mu}, \cdots, e^{-j\pi \frac{(M_x-1)}{2} N_x \mu}]^{\text{T}} \in \mathbb{C}^{M_x}, \\ \boldsymbol{a}_{\mathbb{M}}(\nu) &= [e^{-j\pi \frac{-(M_y-1)}{2} N_y \nu}, \cdots, e^{-j\pi \frac{(M_y-1)}{2} N_y \nu}]^{\text{T}} \in \mathbb{C}^{M_y}. \end{aligned} \quad (4)$$

Similarly, for subarray $\mathbb{N}$, the steering vectors are expressed as

$$\begin{aligned} \boldsymbol{a}_{\mathbb{N}}(\mu) &= [e^{-j\pi \frac{-(N_x-1)}{2} M_x \mu}, \cdots, e^{-j\pi \frac{(N_x-1)}{2} M_x \mu}]^{\text{T}} \in \mathbb{C}^{N_x}, \\ \boldsymbol{a}_{\mathbb{N}}(\nu) &= [e^{-j\pi \frac{-(N_y-1)}{2} M_y \nu}, \cdots, e^{-j\pi \frac{(N_y-1)}{2} M_y \nu}]^{\text{T}} \in \mathbb{C}^{N_y}. \end{aligned} \quad (5)$$

The signals received at subarrays $\mathbb{M}$ and $\mathbb{N}$ at time t can be respectively expressed as

$$\begin{aligned} \boldsymbol{X}_{\mathbb{M}}(t) &= \sum_{l=1}^{L} \alpha_l s(t) \boldsymbol{a}_{\mathbb{M}}(\mu_l) \circ \boldsymbol{a}_{\mathbb{M}}(\nu_l) + \boldsymbol{W}_{\mathbb{M}} \in \mathbb{C}^{M_x \times M_y}, \\ \boldsymbol{X}_{\mathbb{N}}(t) &= \sum_{l=1}^{L} \alpha_l s(t) \boldsymbol{a}_{\mathbb{N}}(\mu_l) \circ \boldsymbol{a}_{\mathbb{N}}(\nu_l) + \boldsymbol{W}_{\mathbb{N}} \in \mathbb{C}^{N_x \times N_y}, \end{aligned} \quad (6)$$

where $\boldsymbol{W}_{\mathbb{M}}$ and $\boldsymbol{W}_{\mathbb{N}}$ are noise matrices associated with subarrays $\mathbb{M}$ and $\mathbb{N}$.

C. Covariance Tensor

The non-uniformity in a coprime array restricts the application of traditional DOA estimation methods. In particular, the well-known spatial smoothing methods [26, 27] cannot be readily applied to such sparse arrays for signal decorrelation when the correlation lags are discontinuous. To address this problem, an array interpolation technique is employed by augmenting virtual sensors at integer multiples of the half-wavelength with the region spanned by the coprime array $\mathbb{S}$ where physical sensors are not present. Several array interpolation methods have been developed [25, 28–30]. In this paper, the coprime array interpolation method developed in [25] is exploited.

The resulting interpolated URA can be expressed as

$$\mathbb{U} = \{(x_{\mathbb{U}}, y_{\mathbb{U}}) \mid x_{\mathbb{U}} \in [-U_x d, U_x d],\ y_{\mathbb{U}} \in [-U_y d, U_y d]\}, \tag{7}$$

where $U_x = \max\left((N_x-1)M_x, (M_x-1)N_x\right)/2$ and $U_y = \max\left((N_y-1)M_y, (M_y-1)N_y\right)/2$ define the utmost sensor positions in the positive X and Y directions, respectively. It is noted that the missing positions bounded by the physical sensors in $\mathbb{S}$ are augmented in $\mathbb{U}$ such that $\mathbb{S} \subset \mathbb{U}$.

The received signals at the interpolated URA $\mathbb{U}$ can be initialized by augmenting the received signals from the 2-D coprime array $\mathbb{S}$ as

$$\langle \boldsymbol{Y}(t) \rangle_{(x_{\mathbb{U}}, y_{\mathbb{U}})} = \begin{cases} \langle \boldsymbol{X}_{\mathbb{M}}(t) \rangle_{(x_{\mathbb{U}}, y_{\mathbb{U}})}, & (x_{\mathbb{U}}, y_{\mathbb{U}})d \in \mathbb{M} \\ \langle \boldsymbol{X}_{\mathbb{N}}(t) \rangle_{(x_{\mathbb{U}}, y_{\mathbb{U}})}, & (x_{\mathbb{U}}, y_{\mathbb{U}})d \in \mathbb{N} \\ 0, & (x_{\mathbb{U}}, y_{\mathbb{U}})d \in \mathbb{U} \backslash \mathbb{S}, \end{cases} \tag{8}$$

with $\langle \cdot \rangle_{(x_{\mathbb{U}}, y_{\mathbb{U}})}$ denoting the element corresponding to the sensor location at $(x_{\mathbb{U}}, y_{\mathbb{U}})d$. We define a binary matrix $\boldsymbol{B}$ to distinguish the virtual and physical sensors in the interpolated URA as

$$\langle \boldsymbol{B} \rangle_{(x_{\mathbb{U}}, y_{\mathbb{U}})} = \begin{cases} 1, & (x_{\mathbb{U}}, y_{\mathbb{U}}) \in \mathbb{S} \\ 0, & (x_{\mathbb{U}}, y_{\mathbb{U}}) \in \mathbb{U} \backslash \mathbb{S}, \end{cases} \tag{9}$$

also denoting its tensor version as $\boldsymbol{\mathcal{B}}$ by replicating the matrix $\boldsymbol{B}$ in additional dimensions.

As such, the initialized signal matrix $\boldsymbol{Y}(t)$ of the 2-D coprime array can be related to the signal matrix of the full URA $\mathbb{U}$ as

$$\boldsymbol{Y}(t) = \boldsymbol{B} \odot \boldsymbol{X}_{\mathbb{U}}(t). \tag{10}$$

The signal matrix of the full URA can be expressed as

$$\boldsymbol{X}_{\mathbb{U}}(t) = \sum_{l=1}^{L} \alpha_l s(t) \boldsymbol{a}_{\mathbb{U}}(\mu_l) \circ \boldsymbol{a}_{\mathbb{U}}(\nu_l) + \boldsymbol{W}_{\mathbb{U}}, \tag{11}$$

where $\boldsymbol{a}_{\mathbb{U}}(\mu)$ and $\boldsymbol{a}_{\mathbb{U}}(\nu)$ are the steering vectors corresponding to the URA $\mathbb{U}$ respectively associated with the X and Y axes, expressed as

$$\begin{aligned} \boldsymbol{a}_{\mathbb{U}}(\mu) &= [e^{-j\pi(-U_x)\mu}, \cdots, e^{-j\pi(U_x)\mu}]^{\mathrm{T}} \in \mathbb{C}^{2U_x+1}, \\ \boldsymbol{a}_{\mathbb{U}}(\nu) &= [e^{-j\pi(-U_y)\nu}, \cdots, e^{-j\pi(U_y)\nu}]^{\mathrm{T}} \in \mathbb{C}^{2U_y+1}. \end{aligned} \tag{12}$$

The covariance tensor of the initialized signal matrix $\boldsymbol{Y}(t)$ is expressed as

$$\begin{aligned} \boldsymbol{\mathcal{R}} = \boldsymbol{\mathcal{B}} \odot \sigma_s^2 \sum_{l=1}^{L} \sum_{l'=1}^{L} \alpha_l^* \alpha_{l'} \boldsymbol{a}_{\mathbb{U}}(\mu_{l'}) \circ \boldsymbol{a}_{\mathbb{U}}(\nu_{l'}) \circ \boldsymbol{a}_{\mathbb{U}}^*(\mu_l) \\ \circ \boldsymbol{a}_{\mathbb{U}}^*(\nu_l) \in \mathbb{C}^{(2U_x+1)\times(2U_y+1)\times(2U_x+1)\times(2U_y+1)}, \end{aligned} \tag{13}$$

where σ_s^2 represents the power of the reference signal. The existence of cross-terms between the coherent signals prevents the covariance tensor from satisfying the conditions of a full-rank CP problem, resulting in tensorial rank deficiency. A particular (u_x, u_y, u_x', u_y')th element of the covariance tensor can be expressed as

$$\begin{aligned} \boldsymbol{\mathcal{R}}(u_x, u_y, u_x', u_y') &= \boldsymbol{\mathcal{B}}(u_x, u_y, u_x', u_y') \\ &\quad \odot \sigma_s^2 \sum_{l'=1}^{L} \alpha_{l'} e^{-j\pi u_x \mu_{l'}} e^{-j\pi u_y \nu_{l'}} \\ &\quad \cdot \sum_{l=1}^{L} \alpha_l^* e^{j\pi u_x' \mu_l} e^{j\pi u_y' \nu_l} \\ &\quad + \sigma_n^2 \zeta_{(u_x, u_y, u_x', u_y')} \\ &= b_{(u_x, u_y)} \sum_{l=1}^{L} \alpha_l^* e^{j\pi u_x' \mu_l} e^{j\pi u_y' \nu_l} \\ &\quad + \sigma_n^2 \zeta_{(u_x, u_y, u_x', u_y')}, \end{aligned} \tag{14}$$

where $u_x, u_x' \in [-U_x, U_x]$ and $u_y, u_y' \in [-U_y, U_y]$, whereas $b_{(u_x, u_y)} = \sigma_s^2 \sum_{l'=1}^{L} \alpha_{l'} e^{-j\pi u_x \mu_{l'}} e^{-j\pi u_y \nu_{l'}}$ depends only on the first two indices (u_x, u_y) of the covariance tensor.

III. DOA Estimation

Sparse array-based DOA estimation for coherent signals poses two significant challenges. One of them is the tensorial rank-deficiency problem. To successfully employ tensor decomposition methods, such as CPD, it is necessary to obtain a full-rank CP problem. Structural tensor reconstruction-based covariance tensor decorrelation is employed in this paper to achieve a full-rank CP model. Second, due to the presence of holes in the difference coarray, the covariance tensor also includes missing entries. These holes in the covariance tensor impede the DOA estimation process and make spatial smoothing inapplicable. To circumvent this issue, we first perform decorrelation of the coherent signals exploiting structural tensor reconstruction, and a low-rank matrix completion technique is employed to fill in the holes. These two steps are described in the following subsections.

A. Decorrelation of Coherent Covariance Tensor via Structural Tensor Reconstruction

To decorrelate the coherent signals in the covariance tensor $\boldsymbol{\mathcal{R}}$, we employ a tensor reconstruction strategy similar to that described in [17]. The objective is to reconstruct a tensorial Toeplitz structure from the covariance tensor $\boldsymbol{\mathcal{R}}$ such that a full-rank (rank L) CP problem is formulated. We consider a pair of indices (u_x, u_y) from the covariance tensor, i.e., $\boldsymbol{\mathcal{R}}(u_x, u_y, :, :)$, which consists of the scaling coefficient $b_{(u_x, u_y)}$ and the components $e^{j\pi u_x' \mu_l}$ and $e^{j\pi u_y' \nu_l}$. A structured tensor $\boldsymbol{\mathcal{D}}_{(u_x u_y)} \in \mathbb{C}^{(U_x+1)\times(U_y+1)\times(U_x+1)\times(U_y+1)}$ is constructed by rearranging the elements from $\boldsymbol{\mathcal{R}}(u_x, u_y, :, :)$. More specifically, the $(-\tilde{u}_x + \tilde{u'}_x)$th row of $\boldsymbol{\mathcal{R}}(u_x, u_y, :, :)$ can be exploited as the $(\tilde{u}_x, :, \tilde{u}_x', :)$th slice of $\boldsymbol{\mathcal{D}}_{(u_x, u_y)}$. Similarly, the $(-\tilde{u}_y + \tilde{u'}_y)$th column of $\boldsymbol{\mathcal{R}}(u_x, u_y, :, :)$ is utilized to construct the $(:, \tilde{u}_y, :, \tilde{u}_y')$th slice of $\boldsymbol{\mathcal{D}}_{(u_x, u_y)}$. In summary, the mapping between $\boldsymbol{\mathcal{R}}(u_x, u_y, :, :)$ and $\boldsymbol{\mathcal{D}}_{(u_x, u_y)}$ can be described as

$$\boldsymbol{\mathcal{D}}_{(u_x, u_y)}(\tilde{u}_x, \tilde{u}_y, \tilde{u}_x', \tilde{u}_y') = \boldsymbol{\mathcal{R}}(u_x, u_y, -\tilde{u}_x + \tilde{u}_x', -\tilde{u}_y + \tilde{u}_y'), \tag{15}$$

where $\tilde{u}_x, \tilde{u}_x' \in [0, U_x]$ and $\tilde{u}_y, \tilde{u}_y' \in [0, U_y]$.

Considering Eqs. (14) and (15), the reconstructed tensor $\boldsymbol{\mathcal{D}}_{(u_x,u_y)}$ can be expressed as

$$\begin{aligned}&\boldsymbol{\mathcal{D}}_{(u_x,u_y)}(\tilde{u}_x,\tilde{u}_y,\tilde{u}'_x,\tilde{u}'_y)\\&\quad= b_{(u_x,u_y)}\sum_{l=1}^{L} e^{j\pi(-\tilde{u}_x+\tilde{u}'_x)\mu_l}\cdot e^{j\pi(-\tilde{u}_y+\tilde{k}'y)\nu_l}.\end{aligned}\tag{16}$$

Neglecting the scaling coefficient $b_{(u_x,u_y)}$, the tensor $\boldsymbol{\mathcal{D}}_{(u_x,u_y)}$ exhibits a tensorial Toeplitz structure in which the cross-terms as those depicted in (13) are eliminated. Accordingly, $\boldsymbol{\mathcal{D}}_{(u_x,u_y)}$ can be reformulated as

$$\boldsymbol{\mathcal{D}}_{(u_x,u_y)} = b_{(u_x,u_y)}\sum_{l=1}^{L}\boldsymbol{g}(\mu_l)\circ\boldsymbol{g}(\nu_l)\circ\boldsymbol{g}^*(\mu_l)\circ\boldsymbol{g}^*(\nu_l),\tag{17}$$

where $\boldsymbol{g}(\mu_l) = [1,\cdots,e^{-j\pi U_x\mu_l}]^{\mathrm{T}} \in \mathbb{C}^{(U_x+1)}$ and $\boldsymbol{g}(\nu_l) = [1,\cdots,e^{-j\pi U_y\nu_l}]^{\mathrm{T}} \in \mathbb{C}^{(U_y+1)}$ act as steering vectors for the lth coherent source in X and Y directions. Eq. (17) is a rank-L CP problem. However, due to the presence of holes in $\boldsymbol{\mathcal{D}}_{(u_x,u_y)}$, we need to interpolate the missing elements of the $\boldsymbol{\mathcal{D}}_{(u_x,u_y)}$ before the CPD method can be applied.

B. Covariance Tensor Recovery via Interpolation

Due to the non-uniform nature of the 2-D coprime array $\mathbb{S}$, the resulting covariance tensor contains holes. The unknown correlations associated with the missing sensors can be estimated through a gridless convex optimization problem. In this subsection, we extend the interpolation method developed in [25], which reconstructs the covariance matrix of a linear sparse array by exploiting the low-rank Hermitian positive semi-definite (PSD) Toeplitz structure of the covariance matrix, to the reconstruction of the underlying covariance tensor of 2-D sparse arrays.

We first matricize the covariance tensor $\boldsymbol{\mathcal{D}}_{(u_x,u_y)}$, denoted as $\boldsymbol{D} \in \mathbb{C}^{(U_x+1)(U_y+1)\times(U_x+1)(U_y+1)}$. Due to the complex scaling factor $b_{(u_x,u_y)}$, the reconstructed covariance tensor $\boldsymbol{\mathcal{D}}_{(u_x,u_y)}$ and, consequently, the matrix $\boldsymbol{D}$ may not be Hermitian in nature. We construct two Hermitian matrices $\boldsymbol{D}_u$ and $\boldsymbol{D}_l$ from matrix $\boldsymbol{D}$ by respectively utilizing the upper and lower triangular elements of $\boldsymbol{D}$ as

$$\begin{aligned}\boldsymbol{D}_u &= \mathrm{triu}(\boldsymbol{D}) + \mathrm{triu}(\boldsymbol{D})^{\mathrm{H}} - \mathrm{Diag}(\mathrm{diag}(\boldsymbol{D}^{\mathrm{H}})),\\ \boldsymbol{D}_l &= \mathrm{tril}(\boldsymbol{D}) + \mathrm{tril}(\boldsymbol{D})^{\mathrm{H}} - \mathrm{Diag}(\mathrm{diag}(\boldsymbol{D}^{\mathrm{H}})).\end{aligned}\tag{18}$$

These two matrices are Hermitian and Toeplitz, thus can be interpolated separately to fill in the missing elements.

Define binary masks denoted by $\boldsymbol{B}_u$ and $\boldsymbol{B}_l$ to distinguish existing and missing entries from the matrices $\boldsymbol{D}_u$ and $\boldsymbol{D}_l$, respectively. The elements of $\boldsymbol{B}_u$ and $\boldsymbol{B}_l$ are 1 for the existing entries and 0 for the missing entries. Recognizing the Hermitian and Toeplitz structure of the two matrices $\boldsymbol{D}_u$ and $\boldsymbol{D}_l$ as well as the low-rank property of the noise-free version of these covariance matrices, the full matrices of $\boldsymbol{D}_u$ and $\boldsymbol{D}_l$ can be recovered by solving the following optimization problems:

$$\begin{aligned}\min_{\boldsymbol{w}_u}\quad & \mathrm{rank}(\mathcal{T}(\boldsymbol{w}_u))\\ \text{s.t.}\quad & \|(\mathcal{T}(\boldsymbol{w}_u))\circ B_u - \boldsymbol{D}_u\|_F^2 \le \delta,\\ & (\mathcal{T}(\boldsymbol{w}_u)) \succeq 0,\end{aligned}\tag{19}$$

and

$$\begin{aligned}\min_{\boldsymbol{w}_l}\quad & \mathrm{rank}(\mathcal{T}(\boldsymbol{w}_l))\\ \text{s.t.}\quad & \|(\mathcal{T}(\boldsymbol{w}_l))\circ B_l - \boldsymbol{D}_l\|_F^2 \le \delta,\\ & (\mathcal{T}(\boldsymbol{w}_l)) \succeq 0,\end{aligned}\tag{20}$$

where δ is an error tolerance.

Due to the NP-hard nature of the problems described in (19) and (20), the rank minimization objective is relaxed by exploiting the nuclear norm minimization. The nuclear norm of $\mathcal{T}(\boldsymbol{w}_1)$ is expressed as $\|\mathcal{T}(\boldsymbol{w}_u)\|_* = \mathrm{Tr}(\sqrt{\mathcal{T}^{\mathrm{H}}(\boldsymbol{w}_u)\mathcal{T}(\boldsymbol{w}_u)})$, and the nuclear norm of $\mathcal{T}(\boldsymbol{w}_l)$ can also be defined in a similar way. As a result, Eq. (19) can be reformulated as

$$\begin{aligned}\min_{\boldsymbol{w}_u}\quad & \|(\mathcal{T}(\boldsymbol{w}_u))\circ B_u - \boldsymbol{D}_u\|_F^2 + \zeta\mathrm{Tr}(\sqrt{T^{\mathrm{H}}(\boldsymbol{w}_u)T(\boldsymbol{w}_u)})\\ \text{s.t.}\quad & (\mathcal{T}(\boldsymbol{w}_u)) \succeq 0,\end{aligned}\tag{21}$$

where ζ is a regularization parameter, and the problem is convex and therefore can be solved. The problem in Eq. (20) can be solved in a similar way.

Using these two interpolated matrices, the missing entries of $\boldsymbol{D}$ is populated, resulting in the filled version denoted as $\tilde{\boldsymbol{D}} \in \mathbb{C}^{(U_x+1)(U_y+1)\times(U_x+1)(U_y+1)}$. Subsequently, the matrix $\tilde{\boldsymbol{D}}$ is rearranged to obtain the interpolated tensor $\tilde{\boldsymbol{\mathcal{D}}}_{(u_x,u_y)} \in \mathbb{C}^{(U_x+1)\times(U_y+1)\times(U_x+1)\times(U_y+1)}$.

C. DOA estimation

Because the interpolated tensor $\tilde{\boldsymbol{\mathcal{D}}}_{(u_x,u_y)}$ is full rank, CPD can be applied on it to estimate the steering vectors $\hat{\boldsymbol{g}}(\mu)$ and $\hat{\boldsymbol{g}}(\nu)$. The estimated $\hat{\mu}$ and $\hat{\nu}$ can then be extracted from the phase of the steering vectors. Finally, the azimuth and elevation angles can be estimated by

$$\begin{aligned}\hat{\theta} &= \arctan\left(\frac{\hat{\nu}}{\hat{\mu}}\right),\\ \hat{\phi} &= \arcsin\left(\sqrt{\hat{\mu}^2+\hat{\nu}^2}\right).\end{aligned}\tag{22}$$

IV. Source Identifiability

The maximum number of identifiable coherent sources using the proposed method relies on the uniqueness of the CPD of $\boldsymbol{\mathcal{D}}_{(u_x,u_y)}$. Denote the estimated CP factor matrices as $\hat{\boldsymbol{G}}(\mu) = [\hat{\boldsymbol{g}}(\mu_1),\hat{\boldsymbol{g}}(\mu_2),\ldots,\hat{\boldsymbol{g}}(\mu_L)]$ and $\hat{\boldsymbol{G}}(\nu) = [\hat{\boldsymbol{g}}(\nu_1),\hat{\boldsymbol{g}}(\nu_2),\ldots,\hat{\boldsymbol{g}}(\nu_L)$, where $\hat{\boldsymbol{g}}(\mu_l)$ and $\hat{\boldsymbol{g}}(\nu_l)$ are the estimated steering vectors. These matrices, along with their conjugates $\hat{\boldsymbol{G}}^*(\mu)$ and $\hat{\boldsymbol{G}}^*(\nu)$, have dimensions $\mathbb{C}^{(U_x+1)\times L}$ and $\mathbb{C}^{(U_y+1)\times L}$, respectively.

The unique estimation of these factor matrices is guaranteed through CPD under the condition [31]:

$$\kappa(\hat{\boldsymbol{G}}(\mu))+\kappa(\hat{\boldsymbol{G}}(\nu))+\kappa(\hat{\boldsymbol{G}}^*(\mu))+\kappa(\hat{\boldsymbol{G}}^*(\nu)) \ge 2L+3,\tag{23}$$

where $\kappa(\hat{\boldsymbol{G}}(\mu)) = \kappa(\hat{\boldsymbol{G}}^*(\mu) = \min(U_x+1, L)$ and $\kappa(\hat{\boldsymbol{G}}(\nu)) = \kappa(\hat{\boldsymbol{G}}^*(\nu) = \min(U_y+1, L)$. To obtain the upper bound of the number of signals to be detected, we consider the scenario of $U_x+1 \le L$ and $U_y+1 \le L$. In this case, Eq. (23) becomes $2U_x+2U_y+4 \ge 2L+3$, i.e., $L \le U_x+U_y+1/2$. Since L takes integer values, the maximum number of coherent sources that can be identified becomes

$$L \le U_x + U_y.\tag{24}$$

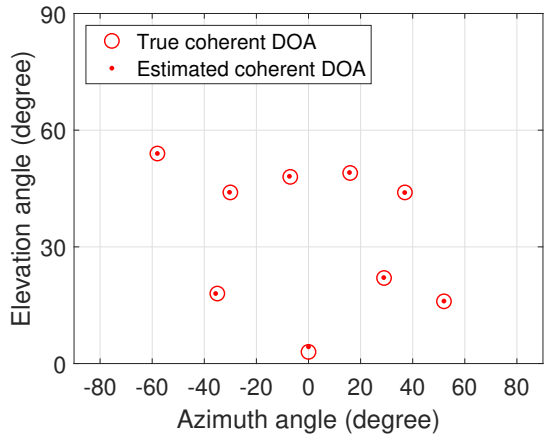

Fig. 2: DOA estimation of coherent sources

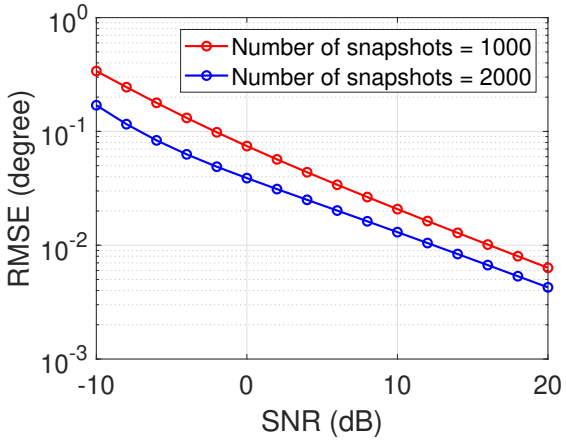

Fig. 3: RMSE vs. input SNR

V. Simulation Results

We consider a 2-D coprime array comprising of two sparse URAs $\mathbb{M}$ and $\mathbb{N}$. The subarray $\mathbb{M}$ consists of $M_x \times M_y = 3 \times 3 = 9$ sensors, while the subarray $\mathbb{N}$ consists of $N_x \times N_y = 5 \times 5 = 25$ sensors. Because the sensor at the origin is shared by both subarrays, the total number of sensors in the 2-D coprime array $\mathbb{S} = \mathbb{M} \cup \mathbb{N}$ is $M_x My + N_x N_y - 1 = 33$. The interpolated URA $\mathbb{U}$ is formed according to Eq. (7), which has dimension $(2U_x+1) \times (2U_y+1) = 13 \times 13$. The proposed approach can therefore detect up to $U_x + U_x = 12$ coherent sources.

To decorrelate the coherence covariance tensor $\boldsymbol{\mathcal{R}}$, we consider the $(1,1)$th slice, i.e., $\boldsymbol{\mathcal{R}}(1,1,:,:) \in \mathbb{C}^{1\times1\times13\times13}$. This slice is arranged according to Eq. (15) to obtain the decorrelated tensor $\boldsymbol{\mathcal{D}}_{(1,1)} \in \mathbb{C}^{7\times7\times7\times7}$. After interpolating the missing entries of $\boldsymbol{\mathcal{D}}_{(1,1)}$, CPD is performed on $\boldsymbol{\mathcal{D}}_{(1,1)}$ to estimate the steering vectors, which are then used to estimate the signal DOAs. We use MATLAB Tensorlab 3 Toolbox [32] to implement CPD on the decorrelated tensor derived through the structural reconstruction approach.

Consider 9 coherent sources with an equal input SNR of 20 dB, and the number of snapshots is 1,000. The azimuth and elevation angles are randomly sampled from uniform distributions with the respective ranges of $-60°$ to $60°$ and $0°$ to $60°$. Fig. 2 depicts the successful detection of all of the coherent sources.

We then evaluate the performance of the proposed approach using root mean-squared error (RMSE) as the performance metric, which is defined as

$$\text{RMSE} = \sqrt{\frac{1}{QL}\sum_{q=1}^{Q}\sum_{l=1}^{L}(\theta_l - \hat{\theta}_{l,q})^2 + (\phi_l - \hat{\phi}_{l,q})^2}, \quad (25)$$

where Q is the number of Monte Carlo trials, and $\hat{\theta}_{l,q}$ and $\hat{\phi}_{l,q}$ are respectively the estimated elevation and azimuth angles of the lth signal in the qth trial. We perform 100 Monte Carlo trials to compute the RMSE values.

Fig. 3 depicts the RMSE results with respect to the input SNR. We consider 5 coherent sources with elevation and azimuth angle pairs being $(54°, -58°)$, $(18°, -35°)$, $(44°, -30°)$, $(48°, -7°)$, $(49°, 16°)$ to compute the RMSE results over a range of input SNR values between -10 dB and 20 dB. The RMSE decreases as the input SNR increases.

VI. Conclusion

In this paper, we proposed a tensor decomposition-based approach for 2-D DOA estimation of coherent sources in sparse arrays. To address the rank-deficiency problem inherent in the coherent covariance tensor, we perform structural tensor reconstruction to reconstruct a Toeplitz covariance tensor. In order to fully utilize the aperture offered by sparse arrays and thereby increase the number of DOFs, we matricize the covariance tensor and enforce the Hermitian structure so that the missing correlations in the reconstructed covariance tensor can be computed through interpolation. The proposed DOA estimation method resolves a high number of coherent signals with enhanced estimation accuracy.

VII. References

[1] H. L. Van Trees, *Optimum Array Processing: Part IV of Detection, Estimation, and Modulation Theory*. Wiley, 2002.

[2] T. E. Tuncer and B. Friedlander, *Classical and Modern Direction-of-Arrival Estimation*. Academic Press, 2009.

[3] Y. Zhang, W. Mu, and M. G. Amin, "Subspace analysis of spatial time-frequency distribution matrices," *IEEE Trans. Signal Process.*, vol. 49, no. 4, pp. 747–759, 2001.

[4] M. G. Amin, X. Wang, Y. D. Zhang, F. Ahmad, and E. Aboutanios, "Sparse array and sampling for interference mitigation and DOA estimation in GNSS," *Proc. IEEE*, vol. 104, no. 6, pp. 1302–1317, June 2016.

[5] S. Sun, A. P. Petropulu, and H. V. Poor, "MIMO radar for advanced driver-assistance systems and autonomous driving: Advantages and challenges," *IEEE Signal Process. Mag.*, vol. 37, no. 4, pp. 98–117, 2020.

[6] S. Sun and Y. D. Zhang, "4D automotive radar sensing for autonomous vehicles: A sparsity-oriented approach," *IEEE J. Sel. Topics Signal Process.*, vol. 15, no. 4, pp. 879–891, 2021.

[7] R. Schmidt, "Multiple emitter location and signal parameter estimation," *IEEE Trans. Antennas Propag.*, vol. 34, no. 3, pp. 276–280, 1986.

[8] R. Roy and T. Kailath, "ESPRIT–estimation of signal parameters via rotational invariance techniques," *IEEE Trans. Acousti., Speech, Signal process.*, vol. 37, no. 7, pp. 984–995, 1989.

[9] J. D. Carroll and J.-J. Chang, "Analysis of individual differences in multidimensional scaling via an N-way generalization of

'Eckart-Young' decomposition," *Psychometrika*, vol. 35, no. 3, pp. 283–319, 1970.

[10] R. A. Harshman, "Foundations of the PARAFAC procedure: Models and conditions for an 'explanatory' multimodal factor analysis," *UCLA Work. Papers Phonetics*, vol. 16, pp. 1–84, 1970.

[11] L. R. Tucker, "Some mathematical notes on three-mode factor analysis," *Psychometrika*, vol. 31, no. 3, pp. 279–311, 1966.

[12] L. De Lathauwer, B. De Moor, and J. Vandewalle, "A multilinear singular value decomposition," *SIAM J. Matrix Anal. Appl.*, vol. 21, no. 4, pp. 1253–1278, 2000.

[13] N. D. Sidiropoulos, R. Bro, and G. B. Giannakis, "Parallel factor analysis in sensor array processing," *IEEE Trans. Signal Process.*, vol. 48, no. 8, pp. 2377–2388, 2000.

[14] H. Zheng, C. Zhou, Z. Shi, Y. Gu, and Y. D. Zhang, "Coarray tensor direction-of-arrival estimation," *IEEE Trans. Signal Process.*, vol. 71, pp. 1128–1142, 2023.

[15] Y. Lin, S. Jin, M. Matthaiou, and X. You, "Tensor-based channel estimation for millimeter wave MIMO-OFDM with dual-wideband effects," *IEEE Trans. Commun.*, vol. 68, no. 7, pp. 4218–4232, 2020.

[16] W. Sun, H. C. So, F. K. W. Chan, and L. Huang, "Tensor approach for eigenvector-based multi-dimensional harmonic retrieval," *IEEE Trans. Signal Process.*, vol. 61, no. 13, pp. 3378–3388, 2013.

[17] H. Zheng, C. Zhou, Z. Shi, and Y. Gu, "Structured tensor reconstruction for coherent DOA estimation," *IEEE Signal Process. Lett.*, vol. 29, pp. 1634–1638, 2022.

[18] P. Pal and P. P. Vaidyanathan, "Nested arrays: A novel approach to array processing with enhanced degrees of freedom," *IEEE Trans. Signal Process*, vol. 58, no. 8, pp. 4167–4181, 2010.

[19] P. P. Vaidyanathan and P. Pal, "Sparse sensing with co-prime samplers and arrays," *IEEE Trans. Signal Process*, vol. 59, no. 2, pp. 573–586, 2010.

[20] S. Qin, Y. D. Zhang, and M. G. Amin, "Generalized coprime array configurations for direction-of-arrival estimation," *IEEE Trans. Signal Process.*, vol. 63, no. 46, pp. 1377–1390, 2015.

[21] P. Pal and P. P. Vaidyanathan, "Coprime sampling and the MUSIC algorithm," in *Proc. Digit. Signal Process. & Signal Process. Educ. Meeting*, Sedona, AZ, 2011, pp. 289–294.

[22] N. Hu, Z. Ye, X. Xu, and M. Bao, "DOA estimation for sparse array via sparse signal reconstruction," *IEEE Trans. Aerosp. and Electron. Syst.*, vol. 49, no. 2, pp. 760–773, 2013.

[23] Y. D. Zhang, M. G. Amin, and B. Himed, "Sparsity-based DOA estimation using co-prime arrays," in *Proc. IEEE Intl. Conf. Acousti., Speech, Signal Process. (ICASSP)*, Vancouver, Canada, May 2013, pp. 3967–3971.

[24] C. Zhou, Y. Gu, Z. Shi, and M. Haardt, "Structured Nyquist correlation reconstruction for DOA estimation with sparse arrays," *IEEE Trans. Signal Process.*, 2023.

[25] C. Zhou, Y. Gu, Z. Shi, and Y. D. Zhang, "Off-grid direction-of-arrival estimation using coprime array interpolation," *IEEE Signal Process. Lett.*, vol. 25, no. 11, pp. 1710–1714, 2018.

[26] T.-J. Shan, M. Wax, and T. Kailath, "On spatial smoothing for direction-of-arrival estimation of coherent signals," *IEEE Trans. Acousti. Speech, Signal Process.*, vol. 33, no. 4, pp. 806–811, 1985.

[27] S. Pillai and B. Kwon, "Forward/backward spatial smoothing techniques for coherent signal identification," *IEEE Trans. Acousti. Speech, Signal Process.*, vol. 37, no. 1, pp. 8–15, 1989.

[28] C.-L. Liu, P. P. Vaidyanathan, and P. Pal, "Coprime coarray interpolation for doa estimation via nuclear norm minimization," in *2016 IEEE Int. Symp. Circuits and Systems (ISCAS)*, Montreal, Canada, 2016, pp. 2639–2642.

[29] C. Zhou, Y. Gu, X. Fan, Z. Shi, G. Mao, and Y. D. Zhang, "Direction-of-arrival estimation for coprime array via virtual array interpolation," *IEEE Trans. Signal Process.*, vol. 66, no. 22, pp. 5956–5971, 2018.

[30] S. Liu, Z. Mao, Y. D. Zhang, and Y. Huang, "Rank minimization-based Toeplitz reconstruction for DoA estimation using coprime array," *IEEE Commun. Lett.*, vol. 25, no. 7, pp. 2265–2269, 2021.

[31] N. D. Sidiropoulos and R. Bro, "On the uniqueness of multilinear decomposition of N-way arrays," *J. Chemometr.*, vol. 14, no. 3, pp. 229–239, 2000.

[32] N. Vervliet, O. Debals, L. Sorber, M. Van Barel, and L. De Lathauwer. Tensorlab 3.0, March 2016. [Online]. Available: https://www.tensorlab.net